

Biomolecule recognition using piezoresistive nanomechanical force probes

Giordano Tosolini, Filippo Scarponi, Salvatore Cannistraro, and Joan Bausells

Citation: *Appl. Phys. Lett.* **102**, 253701 (2013); doi: 10.1063/1.4812469

View online: <http://dx.doi.org/10.1063/1.4812469>

View Table of Contents: <http://apl.aip.org/resource/1/APPLAB/v102/i25>

Published by the AIP Publishing LLC.

Additional information on *Appl. Phys. Lett.*

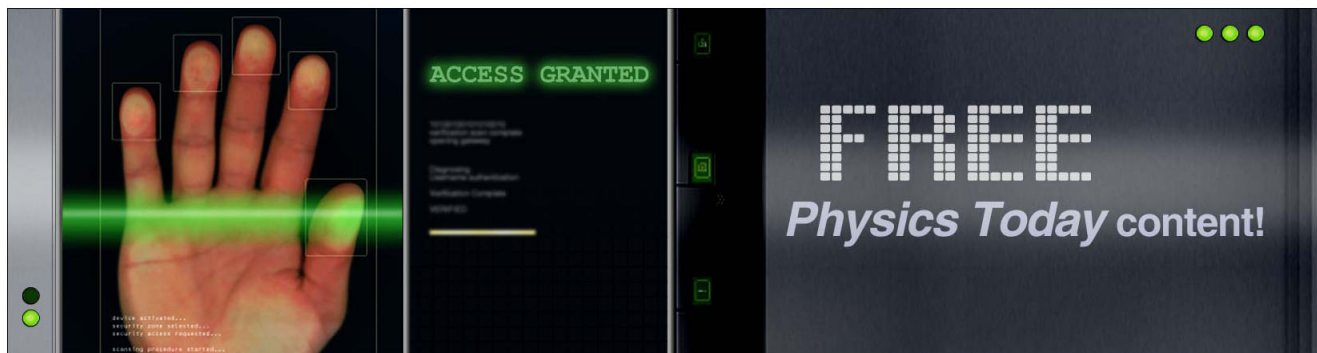
Journal Homepage: <http://apl.aip.org/>

Journal Information: http://apl.aip.org/about/about_the_journal

Top downloads: http://apl.aip.org/features/most_downloaded

Information for Authors: <http://apl.aip.org/authors>

ADVERTISEMENT



Biomolecule recognition using piezoresistive nanomechanical force probes

Giordano Tosolini,¹ Filippo Scarponi,² Salvatore Cannistraro,² and Joan Bausells^{1,a)}

¹Barcelona Microelectronics Institute, IMB-CNM (CSIC), 08193 Bellaterra, Spain

²Biophysics and Nanoscience Centre, CNISM-DEB, Università della Tuscia, Largo dell' Università, 01100 Viterbo, Italy

(Received 24 April 2013; accepted 7 June 2013; published online 26 June 2013)

Highly sensitive sensors are one of the enabling technologies for the biomarker detection in early stage diagnosis of pathologies. We have developed a self-sensing nanomechanical force probe able for detecting the unbinding of single couples of biomolecular partners in nearly physiological conditions. The embedding of a piezoresistive transducer into a nanomechanical cantilever enabled high force measurement capability with sub 10-pN resolution. Here, we present the design, microfabrication, optimization, and complete characterization of the sensor. The exceptional electromechanical performance obtained allowed us to detect biorecognition specific events underlying the biotin-avidin complex formation, by integrating the sensor in a commercial atomic force microscope. © 2013 AIP Publishing LLC. [<http://dx.doi.org/10.1063/1.4812469>]

Biorecognition processes between receptors and their conjugate ligands are very important in biology. These biomolecules can build up very specific complexes displaying a variety of functions such as genome replication and transcription, enzymatic activity, immune response, and cellular signaling. The unambiguous one-to-one complementarity exhibited by these biological partners is widely exploited also in biotechnology to develop biosensors for early stage diagnostic applications in the environmental and biomedical fields.^{1,2} The molecular processes at the basis of biorecognition are driven by forces based on a combination of non-covalent interactions,³ which determine the mechanical and thermodynamic features of the involved complex. Many different techniques are currently used to study the strength and the kinetics of these interactions, both in bulk and at the single molecule level.^{4,5} Among other techniques, a prominent role is played by the atomic force spectroscopy (AFS), in which a biomolecular complex is forced to unbind upon application of a pulling force at nanoscale.^{6,7} This methodology allows probing intra- and intermolecular forces with high sensitivity, in physiological conditions and without labeling. In particular, one interacting biological partner is immobilized on a flat substrate, while the other is covalently attached to an atomic force microscope (AFM) cantilever tip; then the functionalized tip is brought in contact with the substrate and a complex may be formed. Successively, the tip is retracted from the substrate and when the external applied force overcomes the molecular interaction forces, the dissociation takes place and the tip jumps off sharply to a non contact position. Such a jump-off process provides an estimation of the unbinding force, if the cantilever spring constant is known. In the resulting force-distance (F-z) curves, the force is monitored indirectly by measuring the cantilever deflection as detected by a laser focused on the probe and reflected into a position-sensitive photodetector.⁸ Very high resolution down to sub-nanometer and piconewton level is achieved,⁹ thanks to this external optical read-out

method. However, the use of this method is quite time consuming and complicated especially as it regards focusing of the laser on the AFM probe. Moreover, its reliability may result severely hampered in turbid physiological media.

In this respect, the integration of a suitable deflection transducer into the cantilever would allow measurements to be conducted more quickly both in translucent and turbid media, facilitating multiplexing and integration of the system into a fluid cell. Such a device would reveal itself very versatile and could be applied also in a new type of very high sensitive biosensors able to detect even a single molecule, becoming thus important in ultrasensitive detection of biomedical markers for early stage disease diagnosis. Embedding an electrical read-out into the cantilever, such as a resistor^{10,11} or a metal-oxide-semiconductor field effect transistor (MOSFET),^{12,13} exploiting the piezoresistive effect of silicon,^{14,15} can serve to this purpose. In this system, the deflection is measured directly by the resistance variation. Such silicon cantilevers with piezoresistive transduction have been fabricated by Tortonesi *et al.*¹⁰ at the beginning of 1990s. Later, many other research groups used this principle to develop displacement or force sensors for multiple applications: AFM,^{16–19} magnetometry,²⁰ cell mechanics measurements,^{21–23} environmental, chemical and biological sensing,^{24–27} materials and surfaces characterization,^{28,29} etc.^{30,31} Even though Harley and Kenny developed a self-sensing probe capable of a resolution of 0.5 pN in air more than 10 years ago,³⁰ just very recently, Doll and Pruitt fabricated a piezoresistive cantilever, which has a resolution of around 10 pN in liquid environment.³² In order to electrically insulate the sensor, they passivated the dies with 200 nm of parylene only after the end of the batch fabrication process with clear process and mechanical drawbacks.

In this perspective, we have designed self-sensing force probes and we have developed the microfabrication process to obtain batch fabricated nanomechanical cantilevers with embedded piezoresistors, compatible with liquid environment and endowed with sub-10 pN resolution. In Figures 1(a) and 1(b), we report the electrical scheme and a SEM image of the finished device, respectively. These sensors have been optimized for measuring a point force applied at

^{a)} Author to whom correspondence should be addressed. Electronic mail: joan.bausells@imb-cnm.csic.es.

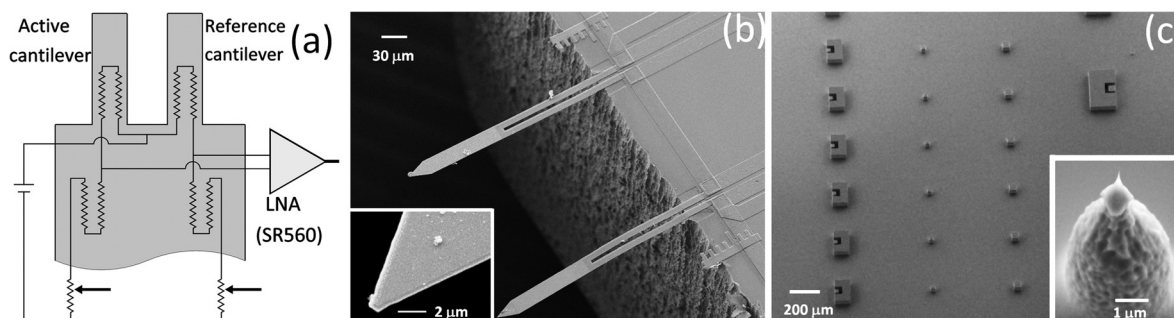


FIG. 1. (a) Sensor electrical scheme. Four piezoresistors are arranged in a $1/4$ active wheatstone bridge configuration: two are embedded into the cantilevers and two into the chip substrate. The bridge can be balanced by two $1\text{ k}\Omega$ potentiometers in series with the substrate resistors. (b) SEM image of the cantilevers and close up of the cantilever end. (c) SEM image of the substrate. Each substrate chip hosts 4 rows of $100\ \mu\text{m}$ high pillars. On the top of each pillar, a $10\ \mu\text{m}$ high tip is defined. The radius of the tip varies between $10\ \text{nm}$ and $300\ \text{nm}$.

the cantilever free end, by using an electromechanical model, reported elsewhere,³³ to estimate the force sensitivity and the electrical noise. The result is that the sensitivity scales proportionally to the piezoresistive factor, inversely to the bending stiffness of the beam and that, to maximize the sensitivity itself, the piezoresistor should be as thin and as far as possible from the neutral axis of the structure. We choose, therefore, to start the microfabrication from a SOI wafer with a $340\ \text{nm}$ thick (100) active layer to reduce as much as possible the bending stiffness and the cantilever spring constant. In view of the need of obtaining a very shallow p-n junction for the piezoresistor, we opted for n-doped silicon, which in addition can offer 45% higher longitudinal piezoresistive factor (π_l) compared to the p-doped silicon.³⁴ For low n-doped silicon, the π_l is maximum for the $\langle 100 \rangle$ crystallographic direction with a value of $102 \times 10^{-11}\ \text{Pa}^{-1}$. Arsenic was chosen for implantation because of its lower penetration range and diffusion coefficient compared to phosphorus. A small dopant diffusion coefficient is very important in this case, since the activation of the impurity is done with a high temperature thermal treatment. Considering these characteristics, arsenic was the best candidate to obtain very shallow p-n junctions. The process has been described in detail elsewhere.^{11,35} In summary, after the implantation of arsenic and the following annealing, the cantilevers were defined by dry etching and interconnected by aluminum. A $100\ \text{nm}$ -thick layer of low stress silicon nitride was deposited to electrically insulate all the conducting areas of the device. Finally, the chip structure was defined by deep reactive ion etching (DRIE) of the bulk silicon from the wafer until reaching the buried oxide (BOX), that was then removed by using a custom made HF vapor etcher.

In order to attain high force resolution, we optimized three different key process steps. A relatively low temperature dopant activation thermal treatment at $950\ ^\circ\text{C}$ for 75 min allowed us to obtain a junction depth of less than $150\ \text{nm}$. A combination of dry etching and wet etching has been used for the back end of line process to avoid any possible damage of the piezoresistors. In addition, we found that the HF vapor provided a fast and quite homogeneous etching across the wafer and that revealed itself as the best option to eliminate completely the oxide. In some chips, the silicon nitride-insulating layer was damaged, yet this process left very clean cantilever surfaces (Fig. 1(b)) in comparison with dry

etching. Although other researchers faced problems related with the BOX cracking during the release process that led to the breaking of the cantilevers,³⁶ we did not encounter similar problems. This is probably due to the protective hard backed photoresist deposited on the component side.

At the same time, substrate chips with sharp tips have been fabricated by a combination of two lithographies, two DRIE and one RIE processes and a final sharpening silicon oxidation.²⁴ In this way, we obtained chips with $10\ \mu\text{m}$ high tips with a curvature radius between $10\ \text{nm}$ and $300\ \text{nm}$ on the top of $100\ \mu\text{m}$ high pillars (Fig. 1(c)). The presence of a sharp tip, which is typically fabricated on the cantilever, is of key importance to perform single molecule AFS experiments.⁶

The electrical, mechanical, and electromechanical characterization of the sensors have been performed completely on the wafer.³³ Figures 2(a) and 2(b) show typical sensitivity and noise power spectral density measurements of a device biased at a constant voltage of $5\ \text{V}$. With the microfabrication process optimization, we obtained probes with a sensitivity of $400 \pm 50\ \mu\text{V}/\mu\text{m}$ and a voltage noise of $3.7 \pm 0.7\ \mu\text{V}$ for the $1\ \text{Hz}$ - $10\ \text{kHz}$ bandwidth with a Hooke factor α of $3 \pm 0.6 \times 10^{-4}$ for the $1/f$ component.³⁷ The noise spectral density of the device immersed in water, shown in Figure 2(b), shows that the silicon nitride layer provides a good insulation for the conductors. The sensor can attain a resolution of $9 \pm 3\ \text{pN}$ (and $14 \pm 4\ \text{nm}$) for the $1\ \text{Hz}$ - $10\ \text{kHz}$ bandwidth by considering a spring constant of $0.62 \pm 0.04\ \text{pN/nm}$, which has been calculated from the measured cantilever dimensions and Young moduli of the materials.³³

Such achieved high force resolution is appropriate to study the interaction involved in the formation of a molecular complex using the AFS measuring approach. For this purpose, highly controlled displacements during the F-z curves are needed and therefore we integrated the sensor into a PicoLe 5100 AFM (Agilent Technologies) to take advantage of the high mechanical stability of this equipment and the highly reliable displacement of the piezo actuator. To this purpose, a custom AFM nose cone (probe holder) was designed and realized by rapid prototyping to allow the positioning of the sensor (Fig. 3(a)). The silicon dies were glued and wire bonded on a custom made $0.4\ \text{mm}$ thick printed circuit board (PCB). On the PCB backside, it was glued also a $0.1\ \text{mm}$ thick steel sheet. All the conductors were passivated

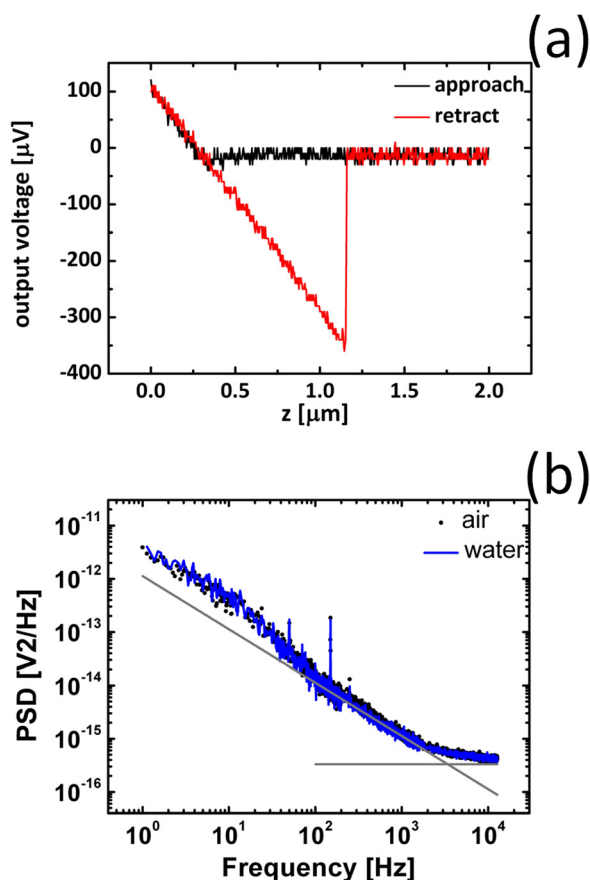


FIG. 2. (a) Sensitivity measurement. An AFM probe performs an F-z curve on the cantilever under test. The approach and retract curves are represented in black and red, respectively: from the slope of the retract curves, we calculate a sensitivity of $394 \mu\text{V}/\mu\text{m}$. (b) Sensor noise power spectral density (PSD) in air. Considering the 1 Hz-10 kHz bandwidth, we have a noise of $3.7 \mu\text{V}$ in air (black) and $3.8 \mu\text{V}$ in water (blue). The Hooke and thermal noise fittings are reported in gray.

by a mono component room temperature curable silicone coating (Dow Corning[®] 3140 RTV). The board was held firmly by a neodymium magnet embedded in the nose cone and inserted into a low profile zero insertion force (ZIF) connector. The sensors were biased by 4 AA rechargeable batteries (Eneloop – Sony) that provided a low noise constant voltage of 5 V, and the output differential voltage was

balanced by two $1 \text{ k}\Omega$ wire wound potentiometers (Fig. 1(a)). This voltage was amplified 2000 times and low pass filtered at 10 kHz by a commercial low noise preamplifier (SR560 – Stanford Research). The resulting signal was used as feedback to approach the cantilever to the sample substrate.

The sensors were tested in de-ionized water (milli-Q water) for several hours in order to verify their performance in liquid medium. Several F-z curves were recorded in order to calculate their sensitivity. Figure 3(b) shows the typical difference between the F-z curves in air and in liquid environment. During the approach in air, there is a jump-to-contact preceded by a region of attractive forces. During the retraction, the restoring force of the cantilever does not exceed the adhesion force and therefore the cantilever remains in contact. In water, instead, there is neither jump-on-contact nor jump-off-contact. As expected, no significant sensitivity variation in liquid respect to air was observed, i.e., $354 \mu\text{V}/\mu\text{m}$ and $359 \mu\text{V}/\mu\text{m}$, respectively. The peak-to-peak noise (Fig. 3(c)) did not change significantly when the liquid was grounded. If the water had floating potential, we noticed instead a relevant increase in the 50 Hz peaks with noise average level rising from $18 \mu\text{V}$ to $42 \mu\text{V}$. These sensitivity and noise values well agree with the values extracted from the on-wafer characterization.

We used this set-up to investigate the biorecognition processes in the well-studied avidin-biotin complex.^{7,38,39} For this purpose, we used a previously developed functionalization procedure.^{35,40} Substrates and cantilevers were cleaned by hot acetone, exposed to UV light, and then covalently functionalized with biotinylated bovine serum albumin (b-BSA) and neutravidin, respectively. In both cases, the proteins were linked to the aldehyde groups of the glutaraldehyde that was linked to the amino groups of the (3-aminopropyl)triethoxysilane (APTES). Non-specific binding sites were blocked by ethanolamine. All the cleanings and functionalizations were performed by immersing the substrate in Petri dishes and the cantilevers into microcapillaries.⁴¹

Just after the functionalization, the sensor and the sample were placed in the nose cone and in the AFM fluid cell, respectively. After pouring $500 \mu\text{l}$ of phosphate buffer saline (PBS) solution (strength of 50 mM and $\text{pH} = 7.5$) into the cell, the cantilever and the substrate were aligned using the

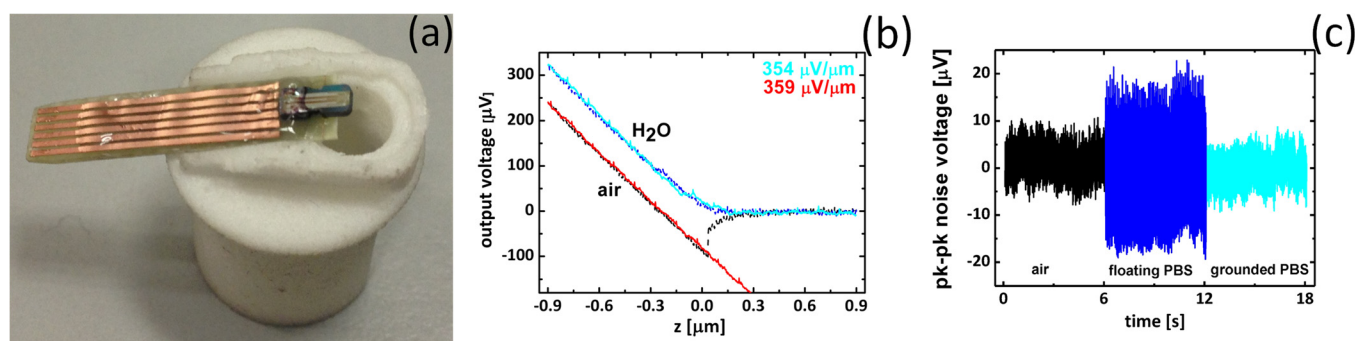


FIG. 3. (a) Force sensor chip onto the nose cone. The die is bonded onto the PCB which is held by a magnet placed into the nose cone. (b) F-z measurement in air (black and red curves) and water (blue and light blue). Approaching the sample in air, a jump-on contact event is detected (black line). Retracting the cantilever for $1 \mu\text{m}$ is not sufficient to overcome the adhesion force, therefore there is no jump-off-contact (red curve). In water, instead, there are no jump phenomena and the sensitivity has no significant variation. From the slopes, we calculated sensitivities of $354 \mu\text{V}/\mu\text{m}$ for air and water environments, respectively. (c) The peak to peak noise has a value of $18 \mu\text{V}$ in air (between 0 and 6 s) and in grounded PBS solution (between 12 and 18 s). When the solution is not grounded (between 6 and 12 s), the noise is more than 2 times higher. There is no significant noise variation between air and grounded PBS.

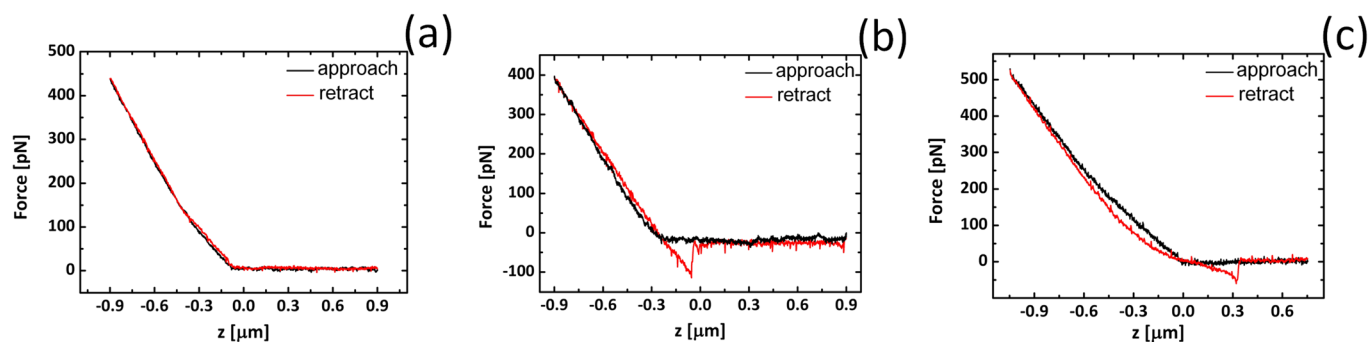


FIG. 4. AFS curves obtained functionalizing the cantilever by b-BSA and the substrate by neutravidin. (a) No event is detected. (b) Non-specific event. The slope of the retract curve is constant before the jump-off. (c) Specific unbinding event between biotin and neutravidin. The slope of the retract curve varies before the jump off. The unbinding force is around 70 pN.

optical microscope and the micromanipulators of the AFM. The cantilever was subsequently engaged to the sample surface, approached further to the sample for $0.9\ \mu\text{m}$ at a constant speed of $1\ \mu\text{m/s}$ for a maximum force of around 500 pN, and after 100 ms, retracted for $1.8\ \mu\text{m}$ at a loading rate of $4.3\ \text{nN/s}$. At the same time, the differential output voltage of the sensor was recorded. Hundreds of curves were acquired for each experiment. In most of them, no unbinding event is visible since the retraction curve follows faithfully the approach curve (Fig. 4(a)). The jump-off event in Figure 4(b) should be attributed to a non-specific adhesion between the substrate and the cantilever since the curve has a constant slope.⁴² In Figure 4(c), instead, the slope is changing before the jump-off-contact. In this case, the average unbinding force resulted to be $44 \pm 12\ \text{pN}$. Unbinding forces between 50 pN and 100 pN for biotin-avidin complex and similar loading conditions have been reported in the literature;⁷ therefore, this value could arise from specific unbinding events occurring between biotin and neutravidin. Due to the fact that the probe spring constant is 3 orders of magnitude lower than the one of the typical probes used in the AFS experiments, the jump-off contact occurs at a length between 200 and 300 nm, which is higher than the literature values.⁷ Anyhow, further improvements in the microfabrication process would enable cantilevers with higher spring constant and sub-10 pN resolution. Finally, it is worth nothing that, in comparison with similar piezoresistive force cantilevers fabricated by other groups, we offer a probe which is compatible with liquid media,³⁰ which has higher resolution^{21,22} and it is produced by more straightforward fabrication process.^{23,32}

In conclusion, we have developed and batch-microfabricated a force sensor based on a cantilever with an embedded piezoresistive transducer, capable of a sub 10 pN resolution (for a bandwidth in the 1 Hz-10 kHz range) in liquid media. We performed single molecule AFS experiments after integrating the sensor into a commercial AFM to take advantages of the mechanical stability and high precision displacement of this equipment. We detected the forces related to the avidin-biotin complex formation, highlighting the possibility of biomolecule label-free recognition in nearly physiological conditions and at single molecule resolution. Beside the very high sensitivity attained, the sensor can be used with no restrictions in opaque media; it can be easily integrated in microfluidic cells and displays a high multiplexing potentiality.

The authors would like to acknowledge IMB-CNM (CSIC) clean room staff for device fabrication. This work has been supported by the Spanish Ministry of Science and Innovation through projects NANOSELECT-CSD2007-00041 (Consolider-Ingenio 2010) and TEC2011-23600, by the European Union through the COST ACTION TD1002 and partly supported by the PRIN-MIUR Project No. 2009 WPZM4S and by AIRC (Grant IG10412).

- ¹A. P. F. Turner, *Chem. Soc. Rev.* **42**, 3184–3196 (2013).
- ²M. M.-C. Cheng, G. Cuda, Y. L. Bunimovich, M. Gaspari, J. R. Heath, H. D. Hill, C. A. Mirkin, A. J. Nijdam, R. Terracciano, T. Thundat, and M. Ferrari, *Curr. Opin. Chem. Biol.* **10**, 11–19 (2006).
- ³I. M. A. Nooren and J. M. Thornton, *EMBO J.* **22**, 3486 (2003).
- ⁴K. C. Neuman and A. Nagy, *Nat. Methods* **5**, 491 (2008).
- ⁵D. Morikis and J. D. Lambris, *Trends Immunol.* **25**, 700 (2004).
- ⁶P. Hinterdorfer and Y. F. Dufrene, *Nat. Methods* **3**, 347 (2006).
- ⁷A. R. Bizzarri and S. Cannistraro, *Dynamic Force Spectroscopy and Biomolecular Recognition* (CRC Press, Boca Raton, 2012).
- ⁸G. Meyer and N. M. Amer, *Appl. Phys. Lett.* **53**, 1045 (1988).
- ⁹J. P. Junker, F. Ziegler, and M. Rief, *Science* **323**, 633 (2009).
- ¹⁰M. Tortoneso, R. C. Barrett, and C. F. Quate, *Appl. Phys. Lett.* **62**, 834 (1993).
- ¹¹G. Villanueva, J. A. Plaza, J. Montserrat, F. Perez-Murano, and J. Bausells, *Microelectron. Eng.* **85**, 1120 (2008).
- ¹²G. Shekhawat, S. H. Tark, and V. P. Dravid, *Science* **311**, 1592 (2006).
- ¹³G. Tosolini, G. Villanueva, F. Perez-Murano, and J. Bausells, *Microelectron. Eng.* **87**, 1245 (2010).
- ¹⁴C. S. Smith, *Phys. Rev.* **94**, 42 (1954).
- ¹⁵A. A. Barlian, W. T. Park, J. R. Mallon, A. J. Rastegar, and B. L. Pruitt, *Proc. IEEE* **97**, 513 (2009).
- ¹⁶R. Linnemann, T. Gotszalk, I. W. Rangelow, P. Dumania, and E. Oesterschulze, *J. Vac. Sci. Technol. B* **14**, 856 (1996).
- ¹⁷Y. Su, A. G. R. Evans, A. Brunnschweiler, G. Ensell, and M. Koch, *Sens. Actuators, A* **60**, 163 (1997).
- ¹⁸R. Jumpertz, A. v. d. Hart, O. Ohlsson, F. Saurenbach, and J. Schelten, *Microelectron. Eng.* **41–42**, 441 (1998).
- ¹⁹J. Thaysen, A. Boisen, O. Hansen, and S. Bouwstra, *Sens. Actuators, A* **83**, 47 (2000).
- ²⁰M. Willemin, C. Rossel, J. Brugger, M. H. Despont, H. Rothuizen, P. Vettiger, J. Hofer, and H. Keller, *J. Appl. Phys.* **83**, 1163 (1998).
- ²¹L. Aeschimann, A. Meister, T. Akiyama, B. W. Chui, P. Niedermann, H. Heinzelmann, N. F. De Rooij, U. Staufer, and P. Vettiger, *Microelectron. Eng.* **83**, 1698 (2006).
- ²²J. Polesel-Mariss, L. Aeschimann, A. Meister, R. Ischer, E. Bernard, T. Akiyama, M. Giazzon, P. Niedermann, U. Staufer, R. Pugin, N. F. De Rooij, P. Vettiger, and H. Heinzelmann, *J. Phys.: Conf. Ser.* **61**, 955 (2007).
- ²³J. C. Doll, A. W. Peng, A. J. Ricci, and B. L. Pruitt, *Nano Lett.* **12**, 6107 (2012).
- ²⁴A. Boisen, O. Hansen, and S. Bouwstra, *J. Micromech. Microeng.* **6**, 58 (1996).

- ²⁵H. Jensenius, J. Thaysen, A. A. Rasmussen, L. H. Veje, O. Hansen, and A. Boisen, *Appl. Phys. Lett.* **76**, 2615 (2000).
- ²⁶P. A. Rasmussen, J. Thaysen, O. Hansen, S. C. Eriksen, and A. Boisen, *Ultramicroscopy* **97**, 371–376 (2003).
- ²⁷A. Choudhury, R. Vujanic, P. J. Hesketh, T. Thundat, and Z. Hu, in *MEMS 2008 IEEE 21st International Conference on Micro Electro Mechanical Systems, Tucson, Arizona, USA, 13-17 January* (IEEE, 2008), p. 228.
- ²⁸B. L. Pruitt and T. W. Kenny, *Sens. Actuators, A* **104**, 68 (2003).
- ²⁹E. Peiner, M. Balke, and L. Doering, *Microelectron. Eng.* **86**, 984 (2009).
- ³⁰J. A. Harley and T. W. Kenny, *Appl. Phys. Lett.* **75**, 289 (1999).
- ³¹J. L. Arlett, J. R. Maloney, B. Gudlewski, M. Muluneh, and M. L. Roukes, *Nano Lett.* **6**, 1000 (2006).
- ³²J. C. Doll and B. L. Pruitt, *J. Micromech. Microeng.* **22**, 095012 (2012).
- ³³G. Tosolini, L. G. Villanueva, F. Perez-Murano, and J. Bausells, *Rev. Sci. Instrum.* **83**, 015002 (2012).
- ³⁴Y. Kanda, *Sens. Actuators A* **28**, 83 (1991).
- ³⁵See supplementary material at <http://dx.doi.org/10.1063/1.4812469> for additional information about the fabrication and functionalization processes.
- ³⁶G. C. Hill, J. I. Padovani, J. C. Doll, B. W. Chui, D. Rugar, H. J. Mamin, N. Harjee, and B. L. Pruitt, *J. Micromech. Microeng.* **21**, 087001 (2011).
- ³⁷J. A. Harkey and T. W. Kenny, *J. Microelectromech. Syst.* **9**, 226 (2000).
- ³⁸V. T. Moy, E. L. Florin, and H. E. Gaub, *Science* **266**, 257 (1994).
- ³⁹S. Izrailev, S. Stepaniants, M. Balsera, Y. Oono, and K. Schulten, *Biophys. J.* **72**, 1568 (1997).
- ⁴⁰A. R. Bizzarri, S. Santini, E. Coppari, M. Bucciattini, S. Di Agostino, T. Yamada, C. W. Beattie, and S. Cannistraro, *Int. J. Nanomed.* **6**, 3011 (2011).
- ⁴¹A. Bietsch, J. Y. Zhang, M. Hegner, H. P. Lang, and C. Gerber, *Nanotechnology* **15**, 873 (2004).
- ⁴²A. R. Bizzarri and S. Cannistraro, *Chem. Soc. Rev.* **39**, 734 (2010).